PHYSICAL REVIEW B VOLUME 35, NUMBER 1 1 JANUARY 1987

Frequency-dependent equation of state of fused silica to 10 GPa

Charles Meade and Raymond Jeanloz
Department of Geology and Geophysics, University of California, Berkeley, California 94720
(Received 25 August 1986)

Using a new technique for optically determining strain in the diamond cell, we have measured the static compression of fused silica and a Ca-Mg-Na glass to over 10 GPa. In our experiments, irreversible compaction of fused silica is precipitated by shear stresses above 10 GPa. For the Ca-Mg-Na glass we observe irreversible compaction beyond 8 GPa under hydrostatic loading. In both glasses we find that the bulk modulus increases sharply at high hydrostatic pressures (~ 11 and ~ 7 GPa, respectively). We show that this increase in bulk modulus can be explained in terms of the transition between relaxed and unrelaxed moduli that is observed at zero pressure, low temperatures, and higher frequencies. Our compression data, measured under quasistatic ($\sim 10^{-4}$ Hz) conditions, are consistent with a wide range of acoustic absorption ($\sim 10^5$–10^{10} Hz) and dielectric loss (10^3–10^4 Hz) measurements in constraining the activation volume for this relaxation process to be $V^* = 7.9 \pm 1.7$ cm^3/mol. We propose that the relaxation involves a change in the compression mechanism, from Si—O—Si bond bending to Si—O bond compression induced either by low temperatures or by high pressure.

I. INTRODUCTION

Fused silica and quartz are both composed of linked SiO_4 tetrahedra, yet the two have profoundly different elastic and thermodynamic properties. Fused silica has a negative or small thermal expansion coefficient,[1] it has two large acoustic absorption peaks at low temperatures,[2] and below 2 K it has a large specific-heat anomaly[3] and small thermal conductivity.[4] Similar anomalies have been found in a wide range of glasses[3,5] and disordered crystals,[6–9] suggesting that these are characteristic properties of the amorphous state.

Roughly, the anomalies can be divided into low- and high-temperature phenomena. A large acoustic and dielectric absorption peak at ~ 50 K in fused silica has been extensively studied between hypersonic and kilohertz frequencies at zero pressure.[10–19] Anderson and Bömmel[10] first proposed that the attenuation was due to thermal relaxation of a group of atoms between two equilibrium configurations in the glass, and they showed that the position of the relaxation peak was well described by a single activation energy over the entire range of experimental data.

Fifteen years later, additional anomalies of excess specific heat,[3] small or negative thermal expansion coefficients,[20] and large values of acoustic absorption[21] were found in fused silica and other glass forming systems below 2 K. Anderson *et al.*[22] were able to reconcile all of these new anomalies with a model of a two-level system (TLS) which couples strongly to thermal and acoustic phonons. They suggested that groups of atoms in the glass could occupy two equilibrium configurations. Phonon-assisted tunneling between the two states then provides a low-temperature mechanism for high acoustic absorption, excess specific heat, and low thermal conductivity. Jäckle *et al.*[23] pointed out that Anderson's TLS model was qualitatively similar to the higher temperature thermal relaxation model, and thus the two may represent relaxation of the same structural unit in the glass but by different processes. While both the TLS and thermal relaxation models have been widely accepted as physically attractive explanations for the elastic and thermodynamic anomalies, and both have been the focus of intense experimental and theoretical interest for the past thirty years, neither has been uniquely correlated with any molecular-scale configuration in an amorphous solid. Moreover, since only the "average" structure of these materials is known, it has been difficult to design experiments which test a model against a particular feature of the glass structure.

In the present study, we have extended the frequency range over which these relaxation processes have been observed by measuring the static compression of fused silica and a Ca-Mg-Na silicate glass to 10 GPa in the diamond cell. As the diamond cell transmits essentially static pressures to the samples, our experiments probe anelastic behavior at long relaxation times and large volume strains. In both glasses, we observe nonelastic deformation and anomalous increases in the bulk modulus at high pressures. We show that our compression data are consistent with a large body of low temperature, high frequency measurements of acoustic attenuation and dielectric loss in silicate glasses. In addition we find that the elastic and anelastic properties of fused silica and crystalline SiO_2 are comparable at equivalent volumes.

II. EXPERIMENTAL METHODS

The experiments were performed with a new optical technique for measuring strain in the diamond cell.[24] Glass samples, approximately 10–20 μm thick and 100 μm across are prepared on one face with a thin (0.1 μm) chromium emulsion mask of ~ 1 μm-wide lines that are spaced 33–65 μm apart. In both experiments, we determine the linear strains at different pressures by optically measuring the change in spacing between the lines on the

glass fragments. The samples were compressed in a gasketted Mao-Bell–type diamond cell with a 4:1 mixture of methanol-ethanol as a pressure medium.[25,26] The pressure is measured with the ruby fluorescence technique[27,28] and remains hydrostatic up to at least 10 GPa. As a check of the hydrostaticity the pressure was measured at four or more points in each run. By monitoring the lack of birefringence in the sample, and by focusing the objective on the upper culet and separately on the sample we check that the sample is not pinched between the diamonds or becoming anisotropic. We note that these are among the first direct equation-of-state measurements of an amorphous material in the diamond cell.

III. RESULTS

A. Fused silica

Linear strains were measured on three separate samples at pressures of up to 15 GPa. The samples were portions of fused-silica photomasks manufactured by Hoya Electronics. Because the glass is isotropic, we can convert measurements of linear strains directly into volume strains. The results for all runs are summarized in Fig. 1 and Table I. The lack of birefringence confirms the assumption of isotropy, and we note that there is little scatter between strains measured on different samples. Sample lengths (l=a given line spacing) are measured before, during, and after compression, and completely reversible elastic strain is obtained on increasing and decreasing pressures to 10 GPa. Above this point the samples suffered irreversible compaction under nonhydrostatic conditions as shown by the hysteresis in three of the decompression measurements to zero pressure. In general, the samples with larger shear stresses show greater compaction.

TABLE I. Compression of fused SiO_2

	V/V_0[a]	Uncertainty	P (GPa)	Uncertainty
Run 1	0.8708	0.0046	4.47	0.10
	0.8196	0.0048	7.00	0.09
	0.8527	0.0039	5.43	0.10
	0.8885	0.0047	3.92	0.02
	0.9978	0.0038	0	0
Run 2	0.9451	0.0045	1.77	0.06
	0.9112	0.0048	2.92	0.05
	0.8210	0.0039	6.64	0.07
	0.7835	0.0036	8.64	0.03
	0.7633	0.0034	10.11	0.15
	0.7543	0.0037	12.90	0.46
	0.8494	0.0038	4.49	0.09
	0.8812	0.0034	2.79	0.04
	0.9377	0.0044	0	0
Run 3	0.9564	0.0040	1.46	0.04
	0.9314	0.0033	2.19	0.08
	0.8901	0.0041	3.79	0.07
	0.8402	0.0041	5.94	0.08
	0.8039	0.0037	7.50	0.10
	0.8798	0.0041	4.09	0.07
	0.9222	0.0037	2.65	0.09
	0.9993	0.0045	0	0
Run 4	0.9536	0.0047	1.59	0.04
	0.9628	0.0050	1.37	0.05
	0.9877	0.0050	0.49	0.05
	0.9913	0.0048	0.31	0.04
	0.9426	0.0046	1.32	0.06
	0.9731	0.0036	0.97	0.04
	0.7604	0.0038	14.58	0.36
	0.9543	0.0040	0	0
Run 5	0.7433	0.0035	11.76	1.16
	0.9157	0.0031	0	0

[a] $V/V_0=(l/l_0)^3$ with subscript zero referring to zero pressure.

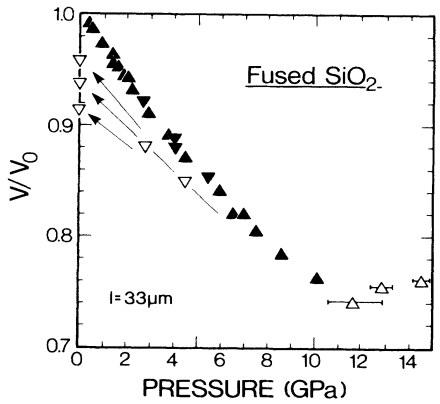

FIG. 1. Volume strain for fused silica as a function of hydrostatic pressure. Up and down pointing triangles indicate measurements on increasing and decreasing pressure. The line spacing is 33 μm. Above 10 GPa nonhydrostatic stresses (error bars) irreversibly compact the samples (open symbols). These runs show hysteresis on decompression, which is schematically shown by the arrows. The final volumes for the compacted samples are plotted at zero pressure.

B. Glass

We carried out a similar compression study on a Ca-Mg-Na glass. The sample was obtained from a low thermal-expansion photomask manufactured by the IMTEC Corporation. Its composition, determined by electron microprobe analysis, is shown in Table II. Its silica content is similar to Pyrex, however it contains a larger amount of calcium, sodium and magnesium relative to aluminum. The deficit in the total for the analysis is

TABLE II. Composition of Ca-Mg-Na glass (in wt. %).

SiO_2	79.60 (0.67)
CaO	5.71 (0.11)
MgO	4.88 (0.08)
Na_2O	4.97 (0.56)
Al_2O_3	1.05 (0.08)
K_2O	0.32 (0.03)
FeO	0.11 (0.02)
ZnO	0.09 (0.05)
Total	96.71

presumably due to the boron content of the glass (3.29% B_2O_3 by difference). Linear strains were measured on three samples at hydrostatic pressures up to 11.6 GPa (Fig. 2, Table III). As before, measurements were made on increasing and decreasing pressures. Although no hysteresis was observed on measurements down to 2.5 GPa, the two recovered samples were compacted ~5% when remeasured at 0 pressure. The transition between elastic and nonelastic behavior is not well defined in these experiments. However, we infer from the observation of hydrostatic pressures, the lack of scatter between measurements, and the similarity with the results for fused silica that our measurements reflect recoverable elastic strains to at least 7 GPa.

IV. DISCUSSION

A. Equations of state for fused silica and Ca-Mg-Na glass

We use Birch's finite-strain formalism to fit the elastic pressure-volume data to a Birch-Murnaghan equation of state.[29] Defining the Eulerian finite strain parameter

$$f=\frac{1}{2}\left[\left(\frac{l_0}{l}\right)^2-1\right] \tag{1}$$

and a normalized pressure

$$F=\frac{P}{3f(1+2f)^{2.5}} \tag{2}$$

we fit the data by a weighted least-squares polynomial for F in terms of f:

$$F=a+bf+cf^2 . \tag{3}$$

In these expressions, P is the experimentally measured pressure and subscript 0 refers to zero-pressure conditions. The coefficients a, b, and c in (3) can be expressed in terms of the zero-pressure bulk modulus (K_0) and its pressure derivatives (K_0',K_0''):

$$\begin{aligned} a&=K_0 , \\ b&=-\tfrac{3}{2}K_0(4-K_0') , \\ c&=\tfrac{3}{2}K_0[K_0K_0''+(K_0'-7)+\tfrac{143}{9}] . \end{aligned} \tag{4}$$

The polynomial expansion of F in terms of f follows directly from the definitions of the strain parameter and normalized pressure, and from a Taylor-series expansion for the compressional energy in terms of f. Second-order polynomials in f, which are fourth order in the strain expansion of the energy, successfully describe the equations of state of many crystalline materials up to large compressions.[30–32] The results for fused silica (Fig. 3) and the Ca-Mg-Na glass (Fig. 4), however, are highly nonlinear, and we find that a weighted quadratic polynomial in f systematically misfits the low-strain (low-weight) points. Higher-order polynomials overfit the data, requiring a larger number of parameters (higher-order derivatives of the bulk modulus) to fit the data than is justified by the number of observations.

Thus, to derive a physically realistic equation of state, which best describes the data with a small number of parameters, we fit the F-versus-f data with quadratic splines. This technique increases the weight of the low-pressure points relative to those at high pressure without overfitting the data to higher-order polynomials.

In a previous paper,[24] we showed that our extrapolated zero pressure values of K_0 and K_0' derived from the hydrostatic measurements are in good agreement with previous ultrasonic studies on fused silica and alkali silicate glasses (Table IV). For fused silica we find $K_0=37\pm5.5$

TABLE III. Compression of Ca-Mg-Na glass.

	V/V_0[a]	Uncertainty	P (GPa)	Uncertainty
Run 1	0.9740	0.0025	0.99	0.07
	0.9477	0.0025	1.84	0.07
	0.9439	0.0026	1.93	0.07
	0.9377	0.0024	2.15	0.08
	0.9163	0.0026	2.88	0.04
	0.8904	0.0026	3.74	0.04
	0.8565	0.0024	5.24	0.07
	0.9261	0.0024	2.52	0.01
Run 2	0.8426	0.0018	6.22	0.06
	0.8389	0.0022	6.49	0.06
	0.8094	0.0021	11.56	0.03
	0.8073	0.0018	11.50	0.07
	0.8223	0.0020	9.78	0.10
	0.8421	0.0023	6.37	0.07
	0.9376	0.0021	0	0
Run 3	0.8298	0.0018	7.63	0.06
	0.8253	0.0024	8.98	0.04
	0.8174	0.0017	10.80	0.14
	0.8768	0.0023	4.42	0.09
	0.9306	0.0024	2.27	0.04
	0.9308	0.0020	0	0

[a] $V/V_0=(l/l_0)^3$ with subscript zero referring to zero pressure.

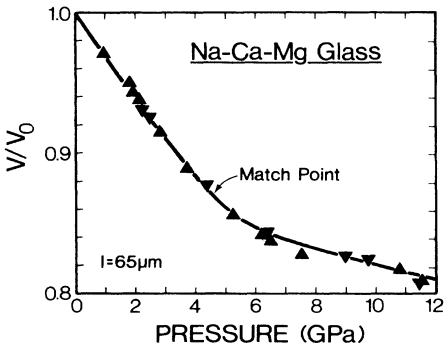

FIG. 2. Volume strain and pressure for Ca-Mg-Na silica glass. Symbols are the same as Fig. 1. The pressure remained hydrostatic up to 11.6 GPa. Strains were measured on decompression to 2.5 GPa, and there was no measurable hysteresis except at zero pressure.

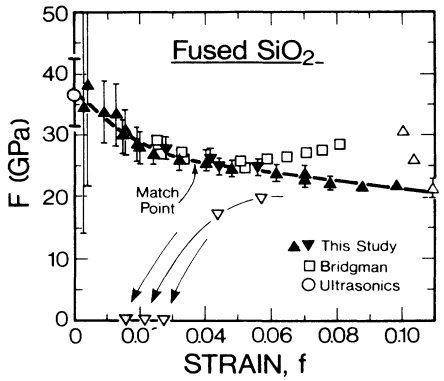

FIG. 3. Normalized pressure F vs strain f for fused silica (see text). Symbols are the same as in Fig. 1. The line represents the room-temperature isotherm (Eulerian fourth-order finite-strain fit to our data). The fit was made with two quadratic splines matched at $f=0.039$. The zero-pressure bulk modulus K_0 is compared with the ultrasonically determined values (open circle). The open squares show the original static-compression data of Bridgman (Ref. 33). On this plot our fit is indistinguishable from the ultrasonically determined equation of state up to 3 GPa. At pressure and on decompression the samples above 10 GPa differ significantly from the equation-of-state fit. In general, the most hydrostatic points show the greatest deviation. The arrows schematically show the decompression of compacted samples. The final compacted volumes are plotted at $F=0$.

and $K_0'=-5.6\pm6.2$. For the Ca-Mg-Na glass the corresponding values are $K_0=35.5\pm3.7$ and $K_0'=-2.9\pm4.1$.

At higher pressures (or strains) the trend in the F-versus-f data is nearly linear, and the equation of state for both glasses can be fitted with greater certainty. In both fits we only include the hydrostatic points. For the Ca-Mg-Na glass, the physical meaning of the fit between 7 and 11 GPa is not clear, as we are measuring nonelastic strain under hydrostatic pressures. However, we include the data in the fit since there is so little scatter between the measurements.

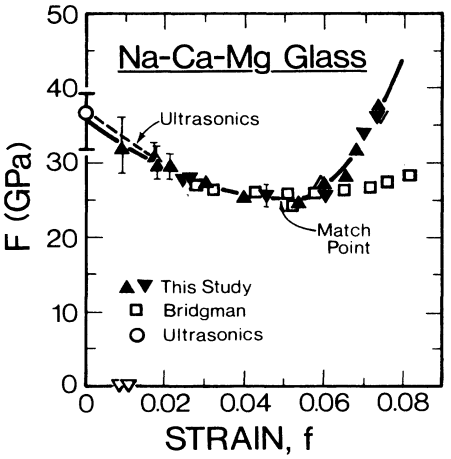

FIG. 4. Normalized pressure F vs strain f for Ca-Mg-Na glass (see text and Fig. 3). The fit was made with two quadratic splines matched at $f=0.050$. The final compacted volumes of the recovered samples are plotted at $F=0$.

TABLE IV. Comparison of zero-pressure K_0 and K_0' values from hydrostatic measurements and ultrasonic studies on fused silica and alkali-metal silicate glass.

	K_0	K_0'	Reference
Fused SiO_2	36.7	−6.3	35
	36.8	−5.9	36
	36.5	−6.2	37
	36.9	−5.3	38
	37.0±5.5	−5.6±6.2	This study
Ca-Mg-Na glass	35.5±3.7	−2.9±4.1	This study

Above 6 GPa our data for fused silica differ significantly from the original compression study of Bridgman.[33] Like our results, however, his extrapolated values of K_0 and K_0' are in good agreement with ultrasonic studies. It is difficult to estimate the sources of discrepancy at higher pressures because there are many uncertainties about Bridgman's sample material and experimental techniques.[34]

From the F-versus-f fits the bulk modulus is given as a function of strain by[29]

$$K=K_0(1+2f)^{5/2}\left[1+f\left[7+\frac{2b}{K_0}\right]-\frac{f^2}{K_0}(9b-3c)+\frac{11cf^3}{K_0}+\cdots\right]. \quad (5)$$

In Figs. 5, 6, and 7 we plot the bulk moduli derived from the fits to our data against pressure and volume. For comparison, we also show the moduli of the crystalline SiO_2 polymorphs. Up to 2 GPa, both glasses show an anomalous decrease in K with pressure. As a negative K_0' has also been measured in ultrasonic[35–38] and Brillouin scattering studies[39,40] on fused silica, we infer from our data that this result is independent of frequency. Similar behavior has also been observed in Pyrex at ultrasonic frequencies.[41]

Above 5 GPa, K increases sharply in the Ca-Mg-Na glass under hydrostatic loading. As there is some nonelastic strain at high hydrostatic pressures our determination of K with (5) is a conservative measure of the bulk modulus above 7 GPa. In fused silica, K does not increase appreciably between 2 and 10 GPa. Above this point, the pressures are not hydrostatic and the glass suffers compaction. However, as shown in Figs. 1 and 3, the more hydrostatic samples appear increasingly incompressible. Thus we infer that K must increase sharply above 11 GPa under hydrostatic loading, as does the Ca-Mg-Na glass at lower pressures, and we have used our most hydrostatic point as a conservative estimate of the bulk modulus to dash the curve above 10 GPa in Fig. 5. We will justify this assumption further in our discussion of anelastic relaxation at high pressure.

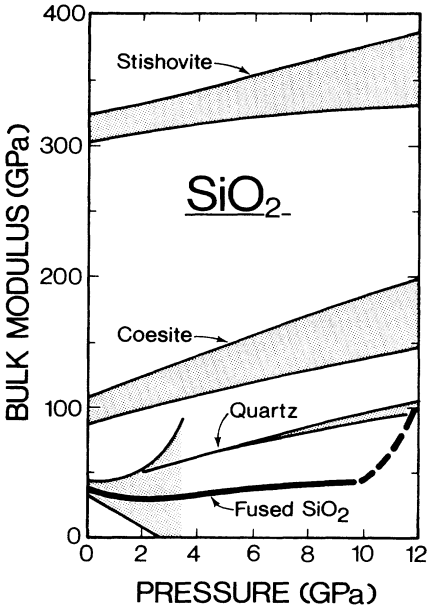

FIG. 5. Bulk modulus of fused silica as a function of pressure determined from our equation-of-state measurements to 10 GPa. Initially, K' is negative and the bulk modulus decreases to a minimum at ~ 2 GPa. Above 10 GPa, the line is dashed to show that the data are consistent with a sharp increase in the bulk modulus. The values for the crystalline SiO_2 polymorphs are shown for comparison (Ref. 63).

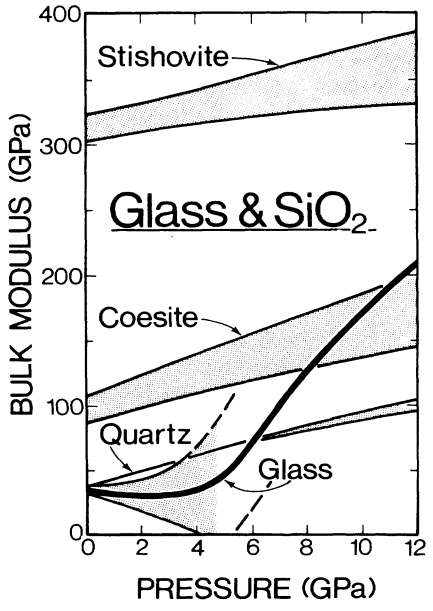

FIG. 6. Bulk modulus of the Ca-Mg-Na glass as a function of pressure determined from our equation of state measurements to 11.6 GPa. K_0' is negative and the minimum in K occurs ~ 2 GPa. The values of the SiO_2 polymorphs are shown for comparison.

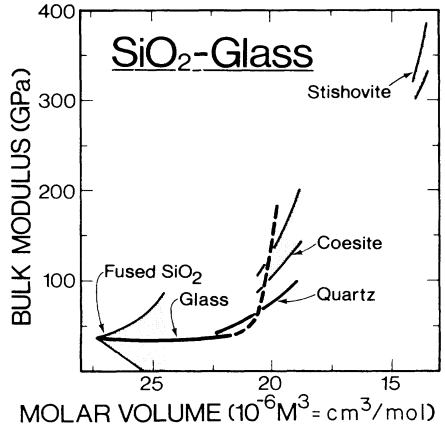

FIG. 7. Bulk modulus of SiO_2 polymorphs and Ca-Mg-Na glass as a function of volume/mole SiO_2. Both glasses show a sharp increase in their bulk moduli at approximately the same volume.

B. Irreversible compaction

In both experiments a few of the samples were irreversibly compacted at high pressures. As shown in Tables I and III the permanent volume strain was approximately $\delta V/V_0 \sim 5\%$. On subsequent examination none of the glasses showed signs of stress birefringence or cracking. At the highest pressures on a run, the strain was repeatedly measured over several days to check for evidence of creep deformation. We were not able to measure any within our resolution ($\sim 10^{-4}$ in linear strain[24]) and thus we interpret the compaction as occurring rapidly upon compression beyond a critical strain.

On decompression, the densified samples appear initially to retrace the compression curves (Figs. 1 and 2), branching off only at low pressures. By comparison, Grimsditch's measurements of Brillouin scattering on fused silica to 17 GPa (Ref. 39) show complete hysteresis on increasing and decreasing pressures. From this result, he argues that the densified glass is a separate amorphous phase of fused silica. Our measurements on decompression show that the compacted samples have a larger bulk modulus than the starting material. This is consistent with the result quoted by Suigura *et al.*[42] of $K_0 \sim 70$ GPa for fused silica compacted to $\rho_0 = 2.6$ g/cm^3.

There is an extensive literature which suggests that shear stresses play an important role in the compaction of silicate glasses,[34,43,44] though in part, this reflects the bias of previous experimental methods which could not achieve large hydrostatic pressures. As all of the earlier compression experiments contained significant but unquantified shear stresses, the relative importance of hydrostatic pressures and shear stresses has not been distinguished. Our measurements on the Ca-Mg-Na glass remained hydrostatic to 11.6 GPa while those on fused silica became nonhydrostatic above 10 GPa. This behavior is consistent with previous observations[45] that the range of hydrostatic pressures in methanol-ethanol depends on the kinetics of the freezing transition above 10

GPa. In all cases, the shear stresses are quantified by measuring the pressure gradients across the samples with the ruby fluorescence technique.

Our data for fused silica suggest that irreversible compaction is indeed precipitated by shear stresses on the sample. This is evident from the scatter between measurements above 10 GPa and the large pressure gradients measured across the samples. Invariably, the samples with the largest shear stresses show the largest compression above 10 GPa, and the largest amount of permanent densification upon recovery to zero pressure.

In the Ca-Mg-Na glass, the transition between elastic and nonelastic behavior is not well defined. In a separate experiment a sample was compressed to 8.54 GPa. The measured pressure in the cell was entirely hydrostatic, yet after decompression the sample showed permanent compaction of 2.43%. Presumably, irreversible compaction occurs under these hydrostatic pressures once the packing of the SiO_4 tetrahedra reaches a critical volume. As the glass has a smaller volume per mole of SiO_2 than fused silica, we would expect the critical volume to occur at a lower pressure. Hence we might observe a similar, hydrostatically induced densification in fused silica at hydrostatic pressures above 10 GPa.

C. Anelastic relaxation

There is a large body of acoustic and dielectric absorption measurements on fused silica over a wide range of frequencies and temperatures.[10–19] The most striking result from this work has been that the relaxation peak measured over eight orders of magnitude in frequency at zero pressure can be characterized by a single activation energy. These data, plotted in Fig. 8, include longitudinal and shear attenuation as well as dielectric loss.

Diamond-cell measurements probe anelastic bulk relaxation at ultralow frequencies. The data of Kondo *et al.*[38] show that bulk attenuation in fused silica shows the same frequency dependence as longitudinal and shear relaxation, and thus we can compare our compression measurements with the data in Fig. 8. From the large number of data at zero pressure, the activation energy, $E^*/k \sim 615$ K, and high-temperature relaxation time, $\tau_0 \sim 2.1 \times 10^{-13}$ s are well constrained. We then use existing data from ultrasonic measurements under pressure[38,46] to find an activation volume, V^* for the relaxation process. We assume that τ_0 determined in the zero pressure measurements is valid at $P > 0$ and fit a line through each data point at pressure. V^* is proportional to the difference between the slopes of these lines and the line describing the zero pressure measurements. By averaging the values for all measurements we find $V^* \sim 7.9 \pm 1.7$ cm^3.

In Fig. 8 we also plot the frequencies ($1.2 \times 10^{-5} < \omega < 2.8 \times 10^{-4}$) and corresponding inverse temperature (293 K) of our "static" compression measurements in the diamond cell. Using the constrained values of E^* and V^* we find that measurements in this frequency range are consistent with a peak in attenuation at 11 GPa. Note that this pressure corresponds to the sharp increase in the bulk modulus under hydrostatic loading. This suggests that the increase in K evident in Figs. 5–7 may be the result of an anelastic transition between a relaxed and unrelaxed modulus.

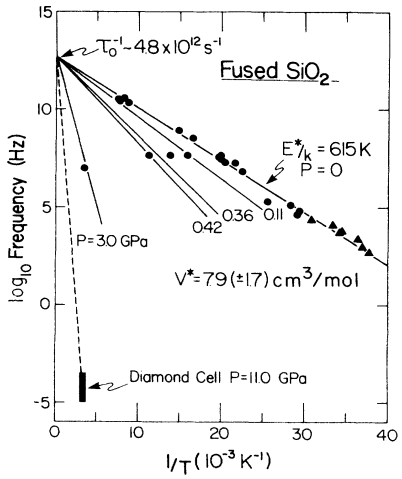

FIG. 8. Inverse temperature of the peak in acoustic attenuation (●) and dielectric loss (△) measurements at different frequencies (Refs. 10–19, 38, and 46). The measurements at zero pressure are used to constrain an activation energy $E^*/k = 614$ K and $\tau_0 = 2.1 \times 10^{-13}$ s. Ultrasonic attenuation measurements at pressure are consistent with an activation volume $V^* = 7.9 \pm 1.7$ cm^3/mole (see text for discussion). The solid lines are the best fit to the published data, showing the trade off between inverse temperature and frequency based on the constrained values of E^* and V^*. The frequencies and temperatures of diamond-cell measurements (this study) are consistent with a peak in bulk attenuation at 11 GPa.

Since there have not been such extensive measurements on silicate glasses, as compared with fused silica, we cannot constrain a value of V^* for the Ca-Mg-Na glass. However, acoustic attenuation[18] and dielectric loss[47] measurements at zero pressure on alkali borosilicate glasses are broadly consistent with our compression results. At a particular temperature, these silica glasses have a longer relaxation time than fused silica. Extrapolating to pressures greater than zero implies that constant frequency measurements should show an attenuation peak at lower pressures than for fused silica. This is in agreement with our determinations of the bulk moduli against pressure for fused silica and the Ca-Mg-Na glass (Figs. 5 and 6).

D. Elastic compression of SiO_2 polymorphs

A wide range of theoretical studies on the tetrahedrally coordinated SiO_2 polymorphs have found that the restoring force for Si—O—Si angle bending is much smaller than for Si—O compression. Lattice dynamical calculations for α-quartz[48] and fused silica,[49] *ab initio* calculations of α-quartz[50] and simple vibrational models of linked SiO_4 tetrahedra[51] are all consistent with a ratio of noncentral to central forces ~ 0.11–0.18.

This disparity has important implications for the elastic properities of crystalline SiO_2 and presumably for fused silica. For example, a systematic increase in K from quartz to coesite to stishovite is accompanied by a shift from Si—O—Si bending to Si—O compression (in the latter case for octahedrally coordinated silicon). X-ray

compression studies of α-quartz[52,53] show that at low pressures volume strain is accommodated by bending of the Si—O—Si angle and concerted rotations of the SiO_4 tetrahedra in threefold symmetry about the c axis. Compression of the SiO_4 tetrahedra may only be important above 6 GPa, beyond the limit of present experiments. In coesite,[54] the relative rotations of the tetrahedra are more constrained by the four membered SiO_4 rings, and the bulk modulus is higher than that of quartz. Up to 6 GPa, strain takes place by compressing the region between rings, bending the Si—O—Si bonds, and direct compression of the SiO_4 tetrahedra. The bulk modulus is extremely large for stishovite since the octahedrally coordinated silicon requires direct straining of the Si—O bond.

Figure 7 shows the bulk moduli against volume per mole of SiO_2 for the two glasses and the SiO_2 polymorphs. The results for the two glasses plot as a single line within the error bars of the fits. There is a broad similarity between the results for the glasses and the crystalline polymorphs: the glasses have comparable bulk moduli to quartz and coesite at comparable volumes. We infer that at high pressures the compression mechanisms are similar at equivalent volumes and thus the increase in K is due to the increasing importance of Si—O compression.

We propose that at low pressures, volume strain is accommodated by compressing the region between tetrahedra as well as bending the Si—O—Si bond. Jorgensen[53] has argued, however, that since the thermal expansion coefficient (α) of fused silica is so much smaller than for α-quartz, the crystal and the glass cannot have similar compression mechanisms (i.e., no Si—O—Si bending). In quartz, thermal expansion takes place by Si—O—Si bending and rotations of the tetrahedra, except at low temperatures where the tetrahedra become constrained and the thermal expansion decreases.[55] Jorgensen proposes that the random glass structure restricts these rotations. Thus, he argues, α-GeO_2 and amorphous GeO_2 have similar values of α since tetrahedral rotations are hindered in elastic compression of the crystal. This match between thermal expansion and elastic compression mechanisms, however, may not be valid between glass and crystal since K is comparable for quartz and fused silica and substantially smaller in amorphous GeO_2 than in α-GeO_2.[56] Extending Jorgensen's argument, the bulk moduli would be larger in the glass since Si—O compression would be important.

In the discussion of Fig. 8, we noted that the sharp increase in K for fused silica at ultralow frequencies and high pressures is consistent with the activation volume and energy of anelastic relaxation at high frequencies. The zero pressure relaxation data are described over eight orders of magnitude by a single activation energy and thus it is not implausible that the anelastic process would persist to the low frequencies of our experiments. Our data also indicate, however, that anelastic relaxation takes place in fused silica at the $P=0$ volume of α-quartz.

At present, there are few constraints on the origin of anomalous low-temperature properties in fused silica. Qualitative models of anelastic relaxation and tunneling states in fused silica, are based either on rotations of the SiO_4 tetrahedra between two configurations[57,58] or oscillations of single oxygen atoms between two silicon atoms.[10,15] Tetrahedral rotations have been observed in quartz near the α-β transition,[59] and may occur in low cristobalite.[60] Experiments have also shown that neutron irradiated quartz displays glasslike, low-temperature anomalies in specific heat, thermal conductivity and acoustic absorption.[7,9] The radiation induced E_1' defect centers appear to be identical in α-quartz and fused silica,[61] however, it is not clear that these are present in nonirradiated glass. In fact, ultrasonic attenuation decreases substantially in neutron irradiated fused silica.[15] From these data Strakna argues that the anelasticity is due to a structural relaxation of oxygen between two silicon atoms in an elongated Si—O—Si bond. Neutron irradiation may destroy these bonds and hence decrease attenuation. Our data do not constrain one particular model, though they do require a mechanism which can be activated at large volume strains.

The sharp increase in K in both fused silica and the Ca-Mg-Na glass indicates that the relaxation strength of our inferred high-pressure bulk attenuation is much larger than the values found at high frequencies, low temperatures, and zero pressure, e.g., Ref. 14. This is consistent with previous ultrasonic studies which have shown that anelastic relaxation in fused silica is strongly pressure dependent. The data of Bartell and Hunklinger[46] show the relaxation strength doubles between 0 and 0.4 GPa at 43 MHz and low temperatures. Also, Kondo *et al.*[38] found a room temperature absorption peak at 3 GPa and 10 MHz that is an order of magnitude larger than comparable measurements at low temperatures and zero pressure. Finally, Raman scattering from fused silica demonstrates a dramatic change in its vibrational properties between 0 and 10 GPa.[62] Presumably this reflects important structural changes, interpreted as a narrowing of the distribution of Si—O—Si angles, and hence concomitant changes in anelastic properties.

V. CONCLUSIONS

Using a new technique for optically determining strain in the diamond cell we measured the static compression of fused silica and a Ca-Mg-Na silicate glass to 10 GPa. In both glasses we observe nonelastic deformation and a sharp increase in the bulk modulus at high pressures. In fused silica this occurs at 11 GPa, just above the hydrostatic limit of our experiments. Shear stresses on these samples at high pressures produced permanent volume strains of up to $\delta V/V_0 \sim 5\%$. In the Ca-Mg-Na glass, the bulk modulus increases sharply above 7 GPa. We have also measured irreversible compaction of this glass at 8 GPa under hydrostatic conditions. We show that the increase in K is consistent with an anelastic transition between a relaxed and unrelaxed modulus. By inverting a wide range of acoustic absorption and dielectric loss measurements we constrain an activation volume (V^*) for the process as $V^* = 7.9 \pm 1.7$ cm^3/mole. Our compression

data are consistent with this result. By transmitting bulk strains under quasistatic conditions, the diamond cell probes relaxation times in the silicate glasses at large volume strains and at ultra long periods of 10^4 s or more.

We find that at high pressures the long-range disorder in the glass does not fundamentally change the elastic properties of SiO_2 relative to the (tetrahedral) crystalline polymorphs. At comparable volumes the glass and crystals have similar bulk moduli. By comparison, our data suggests that the anelastic properties of fused silica and quartz are profoundly different at comparable volumes. We propose that the elastic properties of fused silica are limited by the same compressions mechanisms which are known to be important in the crystalline SiO_2 polymorphs. At low pressure, the glass accommodates volume strain by mutual rotation of the SiO_4 tetrahedra and bending of the Si—O—Si bond. As the volume is reduced, the rotations of the tetrahedra are progressively constrained, forcing strain of the Si—O bond.

ACKNOWLEDGMENTS

The U.C. Berkeley Microelectronics Laboratory supplied the photomasks and E. Knittle provided comments on an earlier manuscript. This work was supported by the National Science Foundation.

[1]G. K. White and J. A. Birch, Phys. Chem. Glasses **6**, 85 (1965).
[2]S. Hunklinger, J. Phys. (Paris) Colloq. **43**, C9-461 (1982).
[3]R. C. Zeller and R. O. Pohl, Phys. Rev. B **4**, 2029 (1971).
[4]J. C. Lasjaunias, A. Ravex, M. Vandorpe, and S. Hunklinger, Solid State Commun. **17**, 1045 (1975).
[5]J. C. Lasjaunias, R. Maynard, and D. Thououze, Solid State Commun. **10**, 215 (1972).
[6]D. A. Ackerman, A. C. Anderson, E. J. Cotts, J. N. Dobbs, W. M. MacDonald, and F. J. Walker, Phys. Rev. B **29**, 966 (1984).
[7]C. Laermans, Phys. Rev. Lett. **42**, 250 (1979).
[8]T. Baumann, M. V. Schickfus, and S. Hunklinger, Solid State Commun. **35**, 587 (1980).
[9]J. W. Gardner and A. C. Anderson, Phys. Rev. B **23**, 474 (1981).
[10]O. L. Anderson and H. E. Bömmel, J. Am. Cer. Soc. **38**, 125 (1955).
[11]J. W. Marx and J. M. Siversten, J. Appl. Phys. **24**, 81 (1953).
[12]A. S. Pine, Phys. Rev. **185**, 1187 (1969).
[13]C. K. Jones, P. G. Klemens, and J. A. Rayne, Phys. Lett. **1**, 31 (1964).
[14]M. E. Fine, H. van Duyne, and N. T. Kenney, J. Appl. Phys. **25**, 402 (1954).
[15]R. E. Strakna, Phys. Rev. **123**, 2020 (1961).
[16]R. Vacher, J. Pelous, F. Plicque, and A. Zarembowitch, J. Non-Cryst. Soc. **45**, 397 (1981).
[17]R. Vacher and J. Pelous, Phys. Rev. B **14**, 823 (1976).
[18]W. W. Scott and R. K. Macrone, Phys. Rev. B **1**, 3515 (1970).
[19]S. H. Mahle and R. D. McCammon, Phys. Chem. Glasses **10**, 220 (1969).
[20]G. K. White, Phys. Rev. Lett. **34**, 204 (1975).
[21]S. Hunklinger, W. Arnold, S. Stein, R. Nava, and K. Dransfeld, Phys. Lett. **A42**, 253 (1972).
[22]P. W. Anderson, B. I. Halperin, and C. Varma, Philos. Mag. **25**, 1 (1972).
[23]J. Jäckle, L. Piché, W. Arnold, and S. Hunklinger, J. Non-Cryst. Soc. **20**, 365 (1976).
[24]C. Meade and R. Jeanloz, in *High Pressure Research in Geophysics and Geochemistry,* edited by M. H. Manghnani and Y. Syono (American Geophysical Union, Washington D.C., 1986).
[25]H. K. Mao, P. M. Bell, K. J. Dunn, R. M. Chrenko, and R. C. Devries, Rev. Sci. Instrum. **50**, 1002 (1979).
[26]J. D. Barnett, S. Block, G. J. Piermarini, Rev. Sci. Instrum. **44**, 1 (1973).
[27]H. K. Mao, P. M. Bell, J. W. Shanez, and D. J. Steinberg, J. Appl. Phys. **49**, 3276 (1978).
[28]H. K. Mao, J. Xu, and P. M. Bell, J. Geophys. Res. **91**, 4673 (1986).
[29]F. Birch, J. Geophys. Res. **83**, 1257 (1978).
[30]E. Knittle and R. Jeanloz, Science **223**, 53 (1984).
[31]E. Knittle, A. Rudy, and R. Jeanloz, Phys. Rev. B **31**, 588 (1985).
[32]D. Heinz and R. Jeanloz, Phys. Rev. B **30**, 6045 (1984).
[33]P. W. Bridgman, Proc. Amer. Acad. Arts Sci. **76**, 55 (1948).
[34]W. Primak, *The Compacted States of Vitreous Silica* (Gordon and Breach, New York, 1975), 184ff.
[35]E. H. Bogardus, J. Appl. Phys. **36**, 2504 (1965).
[36]H. J. McSkimin, J. Acoust. Soc. Am. **29**, 1185 (1957).
[37]L. Peselnick, R. Meister, and W. H. Wilson, J. Phys. Chem. Solids **28**, 635 (1967).
[38]K. Kondo, S. Iio, and A. Sawaoka, J. Appl. Phys. **52**, 2826 (1981).
[39]M. Grimsditch, Phys. Rev. Lett. **52**, 2379 (1984).
[40]J. Schroeder, K. Dunn, and F. Bundy, in *High Pressure in Research and Industry,* Proceedings of the 8th AIRAPT Conference, edited by C. K. Blackman, T. Johannison, and L. Tegner (Arkitektkopia, Uppsala, Sweden, 1982), p. 259.
[41]D. S. Hughes and J. L. Kelly, Phys. Rev. **92**, 1145 (1953).
[42]H. Suigura, K. Kondo, and A. Sawaoka, J. Appl. Phys. **52**, 3375 (1981).
[43]J. D. Mackenzie, J. Am. Cer. Soc. **46**, 470 (1963).
[44]J. Arndt and D. Stoffler, Phys. Chem. Glasses **10**, 117 (1969).
[45]J. M. Besson and J. P. Pinceaux, Rev. Sci. Instrum. **50**, 541 (1979).
[46]U. Bartell and S. Hunklinger, J. Phys. (Paris) Colloq. **43**, C9-489 (1982).
[47]E. M. Amrhein, Glastech. Ber. **42**, 52 (1962).
[48]M. E. Striefler and G. R. Barsch, Phys. Rev. B **12**, 4553 (1975).
[49]R. J. Bell, P. Dean, and D. C. Hubbins-Butler, J. Phys. C **3**, 2111 (1970).
[50]M. D. Newton, M. O'Keefe, and G. V. Gibbs, Phys. Chem. Mineral. **6**, 305 (1980).
[51]F. L. Galeener, A. J. Leadbetter, and M. W. Stringfellow, Phys. Rev. B **27**, 1052 (1983).
[52]L. Levien, C. T. Prewitt, and D. J. Weidner, Am. Mineral. **65**, 920 (1980).
[53]J. D. Jorgensen, J. Appl. Phys. **49**, 4573 (1978).
[54]L. Levien and C. T. Prewitt, Am. Mineral. **66**, 324 (1981).
[55]G. A. Lager, J. D. Jorgensen, and F. J. Rotella, J. Appl. Phys. **53**, 6751 (1982).
[56]J. T. Krause and C. R. Kurkjian, J. Am. Cer. Soc. **51**, 226 (1968).

[57]M. R. Vukcevich, J. Non-Cryst. Soc. **11**, 25 (1972).
[58]L. Guttman and S. Rahman, Phys. Rev. B **33**, 1506 (1986).
[59]G. Van Tendeloo, J. Van LanDuyt, and S. Amelinckx, Phys. Stat. Soc. **33a**, 723 (1976).
[60]D. R. Peacor, Z. Kristallogr. **138**, 274 (1973).
[61]D. L. Griscom, E. J. Friebele, and G. H. Sigel, Solid State Commun. **15**, 479 (1974).
[62]R. J. Hemley, H. K. Mao, P. M. Bell, and B. O. Mysen, Phys. Rev. Lett. **57**, 747 (1986).
[63]J. D. Bass, R. C. Lieberman, D. J. Weidner, and S. J. Finch, Phys. Earth Planet. Inter. **25**, 140 (1981).